Journal of Mathematical Modeling and Fractional Calculus
https://acspublisher.com/journals/index.php/jmmfc
Received:15-12-2025, **Revised:** 21-04-2026,
Accepted: 10-05-2026, **Published:** 20-06-2026,
https://doi.org/10.48165/jmmfc.2026.3105,3(1),1-20 3(1),88-111.

Analytical Investigation of Hopf Bifurcation and Intrinsic Nonlinear Dynamics in a Fractional-Order HIV/AIDS Transmission Framework

Santosh Verma[a*], Ankita Dwivedi[a*]

[a]Guru Ghasidas Vishwavidyalaya (A Central University)Bilaspur - 495009, India.
Corresponding author Email: ankitadwivedi910@gmail.com

Abstract: We propose and analyze a fractional-order HIV/AIDS transmission model that partitions the population into susceptible men and women, undiagnosed and diagnosed infected individuals, AIDS patients, those undergoing treatment, and cumulative mortality. Incorporating demographic and epidemiological data from South Africa and India, parameter estimates are adjusted to capture regional variations in HIV prevalence and treatment coverage. The model ensures biological plausibility by demonstrating the positivity and boundedness of all solutions. The disease-free and endemic equilibrium states are derived, with the basic reproduction number R_0 formulated through the next-generation matrix approach. Stability analysis both local and global are conducted using RouthŰHurwitz criteria, and conditions for Hopf bifurcation are identified to reveal potential oscillatory infection dynamics. The existence and uniqueness of solutions are assured under a Lipschitz condition. Overall, this framework offers a rigorous mathematical foundation for understanding HIV transmission mechanisms and informing intervention strategies in heterogeneous populations.
Keywords: Caputo Fractional-Order HIV/AIDS Model, Fractional order epidemic model, Stability, Basic Reproduction Number, Hopf bifurcation

1. Introduction

Human Immunodeficiency Virus (HIV) remains a substantial global health challenge, affecting millions and contributing to a continual rise in new infections each year [3, 24]. Mathematical modeling has proven invaluable for elucidating HIV/AIDS transmission pathways and evaluating public health strategies for control and treatment [19, 21]. Conventional integer-order differential models have advanced our understanding of disease progression but typically fail to account for the memory and hereditary characteristics intrinsic to biological systems [17, 27, 28]. The emergence of fractional calculus has introduced new possibilities for modeling epidemiological phenomena. By incorporating memory effects and long-range dependencies, fractional-order derivatives provide a more accurate and flexible framework for describing the complex temporal behaviors found in HIV transmission [5, 7, 16, 23, 25, 28]. The Caputo fractional derivative, in particular, is often selected for biological modeling due to its compatibility with initial conditions based on physical reality [5, 7]. Hopf bifurcation analysis is essential for understanding qualitative shifts within epidemic systems. When the basic reproduction number $\mathscr{R}_0$ crosses a threshold, bifurcation can occur, triggering oscillatory dynamics, periodic outbreaks, or complex temporal responses [27, 29]. In HIV, oscillating immune responses and fluctuations in viral load have been observed in clinical settings, reinforcing the importance of bifurcation theory [4, 12, 20, 22, 32, 33].

Prior studies indicate that fractional-order dynamics can significantly affect epidemic bifurcation behavior delaying, altering, or suppressing bifurcation onset, reshaping equilibrium stability, and influencing the persistence of the disease [10, 14, 15, 26, 30]. Further, adding treatment and control interventions into fractional-order HIV models fosters the development of more robust and realistic strategies for epidemic management [10, 14, 26].The graphs were plotted using Python based on the data presented in Tables (1, 2, and 3).

1.1. Motivation:

Despite extensive research using integer-order models, the exploration of Hopf bifurcation in fractional-order HIV/AIDS transmission models remains limited. Real-world HIV dynamics are often Non-Markovian, with immune and viral populations exhibiting memory effects best captured by fractional order approaches. To make progress in understanding complex epidemic patterns and devising effective interventions, it is crucial to investigate models that account for these features.

1.2. Novelty

This work fills an important gap by systematically investigating the Hopf bifurcation phenomena in a fractional-order HIV/AIDS model, particularly focusing on how fractional dynamics influence stability boundaries and the emergence of oscillatory behavior. The main novelties include:

- Demonstrating how the fractional order parameter modifies the threshold conditions for Hopf bifurcation, thereby affecting the persistence and oscillatory nature of the disease dynamics.
- Providing a comprehensive analytical study of stability and bifurcation combined with rigorous numerical simulations to capture and visualize complex behaviors unique to fractional-order epidemiological systems.

The rest of the paper proceeds as follows: Section 1 introduces the mathematical formulation of the fractional order HIV/AIDS model, Section 2 preliminaries, Section 3 Analysis of the Model, Section 4 non negativity and uniform boundedness Section 5 details the stability analysis, Section 6 basic reproduction number, Section 7 derivation of hopf bifurcation conditions. Section 8 presents numerical simulations and diagrams.

2. Preliminaries

The Caputo fractional derivative of order $\alpha \in (0,1)$ for a sufficiently smooth function $f(t)$ is defined by

$$ {}^{C}D_t^{\alpha} f(t) = \frac{1}{\Gamma(1-\alpha)} \int_0^t \frac{f'(\tau)}{(t-\tau)^{\alpha}}\, d\tau, \tag{1} $$

where $\Gamma(\cdot)$ denotes the Gamma function and $f'(\tau)$ is the first derivative of f with respect to τ. This definition extends the classical derivative to fractional orders, allowing the incorporation of memory and hereditary effects into mathematical models. It is particularly suitable for applications in physical and biological systems, as it permits the use of standard initial conditions expressed in terms of integer-order derivatives. Some fundamental properties of the Caputo fractional derivative are as follows:

- The derivative of a constant function is zero:

$$ {}^{C}D_t^{\alpha} c = 0. $$

- For a power function $f(t) = t^{\beta}$ with $\beta > \alpha - 1$, we have

$$ {}^{C}D_t^{\alpha} t^{\beta} = \frac{\Gamma(\beta+1)}{\Gamma(\beta-\alpha+1)} t^{\beta-\alpha}. $$

- For the exponential function $f(t) = e^{\lambda t}$, the fractional derivative can be expressed in terms of special functions and reflects memory-dependent growth behavior:

$$ {}^{C}D_t^{\alpha} e^{\lambda t} = \lambda^{\alpha} e^{\lambda t}, \quad \text{under suitable conditions.} $$

The Caputo derivative requires that the function f be at least once differentiable, which facilitates its application in problems where classical initial conditions are prescribed. This formulation differs from the Riemann–Liouville fractional derivative, which is defined via fractional integrals and is generally less convenient for handling standard initial conditions in applied models. Standard references for these definitions and properties include Podlubny (1999) [3] and other classical texts in fractional calculus [7, 16, 28].

2.1. Model Formulation

The fractional-order HIV model [9] is given by the following system of equations, where $0 < \tau \leq 1$ denotes the order of the Caputo fractional derivative:

$$\begin{cases} {}_{C_0}D_t^{\tau} S_1 &= (1-\chi)\,\omega - \Theta_1 S_1 I_1 - \zeta S_1 - \Theta_3 S_1 I_2, \\ {}_{C_0}D_t^{\tau} S_2 &= d\theta - \Theta_2 S_2 I_1 - \zeta S_2 - \Theta_4 S_2 I_2, \\ {}_{C_0}D_t^{\tau} I_1 &= \Theta_1 S_1 I_1 + \Theta_2 S_2 I_1 - \upsilon I_1 - \sigma I_1 - \zeta I_1, \\ {}_{C_0}D_t^{\tau} I_2 &= \upsilon I_1 - \tau I_2 - \varphi I_2 - \zeta I_2 + \Theta_3 S_1 I_2 - \Theta_4 S_2 I_2, \\ {}_{C_0}D_t^{\tau} A &= \sigma I_1 - \varphi I_2 - \rho T - \varpi_1 A - \zeta A, \\ {}_{C_0}D_t^{\tau} T &= \tau I_2 - \rho T - \zeta T - \varpi_2 T, \\ {}_{C_0}D_t^{\tau} D &= \zeta(I_1 + I_2 + A + T) + \varpi_1 A + \varpi_2 T. \end{cases} \tag{2}$$

The fractional-order HIV/AIDS transmission model uses the Caputo derivative $0 < \tau \leq 1$ to incorporate memory effects, making current infection dynamics dependent on past states. The population is divided into seven compartments: $S_1, S_2, I_1, I_2, A, T, D$, representing susceptible (aware/unaware), infected (aware/unaware), AIDS patients, treatment, and deaths. Awareness and treatment influence transitions between compartments, with infection driven by $\Theta_1, \Theta_2, \Theta_3, \Theta_4$ and natural mortality ζ. When $\tau = 1$, the model reduces to its classical form, enabling analysis of persistence, thresholds, and stability using fractional calculus.

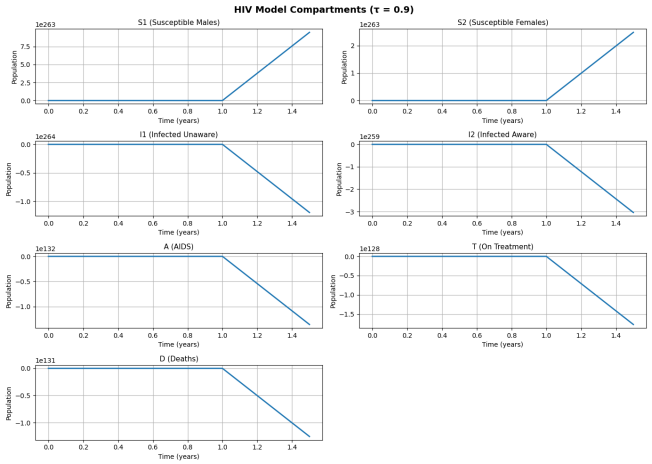

Figure 1: HIV model Compartment ($\tau = 0.9$)

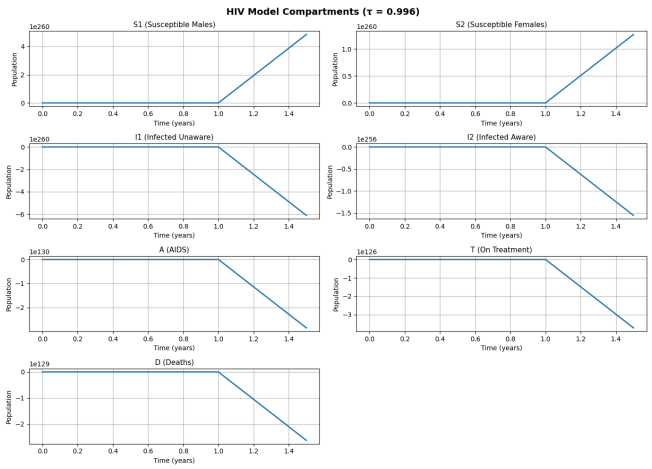

Figure 2: HIV model Compartment ($\tau = 0.996$)

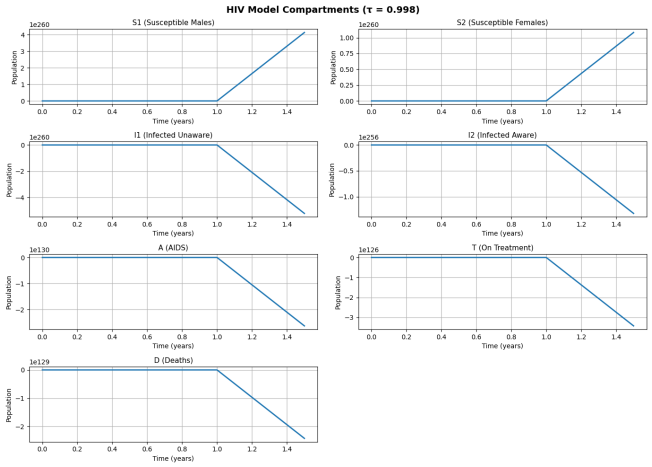

Figure 3: HIV model Compartment ($\tau = 0.998$)

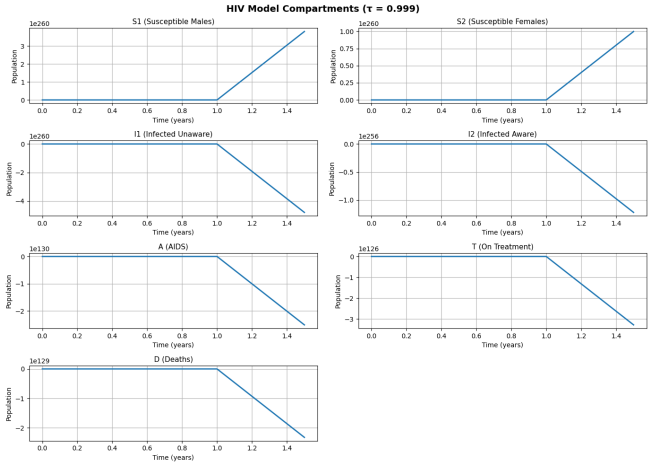

Figure 4: HIV model Compartment ($\tau = 0.999$)

In Figure (1, 2, 3, 4) its illustrate the dynamics HIV model compartment with $\tau = 0.9, 0.996, 0.998, 0.999$.

3. Analysis of the Model

This section examines the mathematical soundness of the proposed model, emphasizing the conditions for existence and uniqueness of solutions, along with ensuring the positivity and bounded nature of all system variables [1, 2, 3].

Existence and Uniqueness

Theorem 3.1. *There exists a unique solution of he proposed model eq.(2) for each non-negative condition.*

Proof. We are seeking for a sufficient condition for the presence and uniqueness of the proposed model solutions in the region $\Theta \times [0, \mathscr{T}]$, where $\Theta = (S_1, S_2, I_1, I_2, A, T, D) \in \mathbb{R}^7 from : \max ||S_1||, ||S_2||, ||I_1||, ||I_2||, ||T||, ||D||$. The method employed is used consider a mapping

$\mathscr{F}(Y) = \mathscr{F}_1(Y), \mathscr{F}_2(Y), \mathscr{F}_3(Y), \mathscr{F}_4(Y), \mathscr{F}_5(Y), \mathscr{F}_6(Y), \mathscr{F}_7(Y)$. Where $Y = (S_1, S_2, I_1, I_2, A, T, D)$ and $\hat{Y} = (\hat{S_1}, \hat{S_2}, \hat{I_1}, \hat{I_2}, \hat{A}, \hat{T}, \hat{L}$

$$
\begin{aligned}
\mathscr{F}_1(Y) &= (1-\chi)\,\omega - \Theta_1 S_1 I_1 - \zeta S_1 - \Theta_3 S_1 I_2,\\
\mathscr{F}_2(Y) &= d\theta - \Theta_2 S_2 I_1 - \zeta S_2 - \Theta_4 S_2 I_2,\\
\mathscr{F}_3(Y) &= \Theta_1 S_1 I_1 + \Theta_2 S_2 I_1 - \upsilon I_1 - \sigma I_1 - \zeta I_1,\\
\mathscr{F}_4(Y) &= \upsilon I_1 - \tau I_2 - \varphi I_2 - \zeta I_2 + \Theta_3 S_1 I_2 - \Theta_4 S_2 I_2,\\
\mathscr{F}_5(Y) &= \sigma I_1 - \varphi I_2 - \rho T - \varpi_1 A - \zeta A,\\
\mathscr{F}_6(Y) &= \tau I_2 - \rho T - \zeta T - \varpi_2 T,\\
\mathscr{F}_7(Y) &= \zeta(I_1 + I_2 + A + T) + \varpi_1 A + \varpi_2 T.
\end{aligned}
$$

$$
\begin{aligned}
||\mathscr{F}(Y) - \mathscr{F}\hat{Y}|| = \Bigg\{ & |\mathscr{F}_1(Y) - \mathscr{F}_1\hat{Y}| + |\mathscr{F}_2(Y) - \mathscr{F}_2\hat{Y}| + |\mathscr{F}_3(Y) - \mathscr{F}_3\hat{Y}| + |\mathscr{F}_4(Y) - \mathscr{F}_4\hat{Y}|\\
& + |\mathscr{F}_5(Y) - \mathscr{F}_5\hat{Y}| + |\mathscr{F}_6(Y) - \mathscr{F}_6\hat{Y}| + |\mathscr{F}_7(Y) - \mathscr{F}_7\hat{Y}| +\\
& = |(1-\chi)\,\omega - \Theta_1 S_1 I_1 - \zeta S_1 - \Theta_3 S_1 I_2 - (1-\chi)\,\omega + \Theta_1 \hat{S_1}\hat{I_1} + \zeta \hat{S_1} + \Theta_3 \hat{S_1}\hat{I_2}|\\
& + |d\theta - \Theta_2 S_2 I_1 - \zeta S_2 - \Theta_4 S_2 I_2 - d\theta + \Theta_2 \hat{S_2}\hat{I_1} + \zeta \hat{S_2} + \Theta_4 \hat{S_2}\hat{I_2}|\\
& + |\Theta_1 S_1 I_1 + \Theta_2 S_2 I_1 - \upsilon I_1 - \sigma I_1 - \zeta I_1 - \Theta_1 \hat{S_1}\hat{I_1} - \Theta_2 \hat{S_2}\hat{I_1} + \upsilon \hat{I_1} + \sigma \hat{I_1} + \zeta \hat{I_1}| +\\
& |\upsilon I_1 - \tau I_2 - \varphi I_2 - \zeta I_2 + \Theta_3 S_1 I_2 - \Theta_4 S_2 I_2 - \upsilon \hat{I_1} + \tau \hat{I_2} + \varphi \hat{I_2} + \zeta \hat{I_2}\\
& - \Theta_3 \hat{S_1}\hat{I_2} + \Theta_4 \hat{S_2}\hat{I_2}|\\
& + |\sigma I_1 - \varphi I_2 - \rho T - \varpi_1 A - \zeta A - \sigma \hat{I_1} + \varphi \hat{I_2} + \rho \hat{T} + \varpi_1 \hat{A} + \zeta \hat{A}|\\
& + |\tau I_2 - \rho T - \zeta T - \varpi_2 T - \tau \hat{I_2} + \rho \hat{T} + \zeta \hat{T} + \varpi_2 \hat{T}|\\
& + |\zeta(I_1 + I_2 + A + T) + \varpi_1 A + \varpi_2 T - \zeta(\hat{I_1} + \hat{I_2} + \hat{A} + \hat{T}) - \varpi_1 \hat{A} - \varpi_2 \hat{T}|.\\
& - \Theta_1 S_1 I_1 - \zeta S_1 - \Theta_3 S_1 I_2 + \Theta_1 \hat{S_1}\hat{I_1} + \zeta \hat{S_1} + \Theta_3 \hat{S_1}\hat{I_2}\\
& \leq \Theta_1\,|S_1 I_1 - \hat{S_1}\hat{I_1}| + \zeta |S_1 - \hat{S_1}| + \Theta_3\,|S_1 I_2 - \hat{S_1}\hat{I_2}|\\
& \leq \Theta_1 \big(M|I_1 - \hat{I_1}| + M|S_1 - \hat{S_1}|\big) + \zeta |S_1 - \hat{S_1}| + \Theta_3 \big(M|I_2 - \hat{I_2}| + M|S_1 - \hat{S_1}|\big)\\
& = (\Theta_1 M + \zeta + \Theta_3 M)|S_1 - \hat{S_1}| + \Theta_1 M |I_1 - \hat{I_1}| + \Theta_3 M |I_2 - \hat{I_2}|
\end{aligned}
\tag{3}
$$

$$
\|\mathscr{F}(Y) - \mathscr{F}(\hat{Y})\| = \sum_{\text{components}} c_j\,|(y_j - \hat{y}_j)| \;\leq\; \Big(\max_j c_j\Big) \sum_{\text{components}} |y_j - \hat{y}_j|. \tag{4}
$$

$$
\begin{aligned}
c_{S_1} &= 2M(\Theta_1 + \Theta_3) + \zeta,\\
c_{S_2} &= 2M(\Theta_2 + \Theta_4) + \zeta,\\
c_{I_1} &= 2M(\Theta_1 + \Theta_2) + 2\sigma + 2\upsilon + 2\zeta,\\
c_{I_2} &= 2M(\Theta_3 + \Theta_4) + 2\tau + 2\varphi + 2\zeta,\\
c_A &= 2\varpi_1 + 2\zeta,\\
c_T &= 2\rho + 2\varpi_2 + 2\zeta.
\end{aligned}
\tag{5}
$$

$$
\|\mathscr{F}(Y) - \mathscr{F}(\hat{Y})\| \;\leq\; L\|Y - \hat{Y}\|, \qquad L = \max\{c_{S_1}, c_{S_2}, c_{I_1}, c_{I_2}, c_A, c_T\}. \tag{6}
$$

where $\mathscr{F}(Y)$ is the collection of nonlinear and linear terms present in the system. This final expression provides a Lipschitz type inequality. Such an inequality is instrumental in establishing uniqueness, stability, or convergence bounds for fractional-order systems. □

4. Non-negativity and Uniform Boundedness of Solutions

We analyze the HIV transmission model using a fractional-order system of differential equations, where the derivative order satisfies $0 < \tau \leq 1$.

Theorem 4.1 (Non-negativity)**.** *If the initial conditions satisfy*

$$
S_1(0), S_2(0), I_1(0), I_2(0), A(0), T(0), D(0) \geq 0,
$$

then the solutions $S_1(t), S_2(t), I_1(t), I_2(t), A(t), T(t), D(t)$ remain non-negative for all $t \geq 0$ [4, 5, 6].

Proof. Each equation's inflow terms are non-negative, while outflow terms are proportional to the state variables themselves. When a state variable reaches zero, its derivative is non-negative, preventing it from becoming negative. Hence, the solution remains in the non-negative orthant. □

Theorem 4.2 (Uniform Boundedness)**.** *The total population*

$$N(t) = S_1(t) + S_2(t) + I_1(t) + I_2(t) + A(t) + T(t)$$

is uniformly bounded [7, 8, 9], satisfying

$$N(t) \leq \frac{\pi_\tau}{\mu_\tau}, \quad \textit{for all } t \geq 0.$$

Proof. Summing the system equations yields

$$C_0 D_t^\tau N(t) \leq \pi_\tau - \mu_\tau N(t).$$

Solving this inequality using the Mittag-Leffler function shows that $N(t)$ is bounded above by $\frac{\pi_\tau}{\mu_\tau}$ as $t \to \infty$. □

5. Stability Analysis

This section investigates the stability of equilibrium points in the fractional order HIV/AIDS model. Both local and global stability properties are analyzed to understand the long-term behavior of the system under varying conditions [14, 30, 32].

Steady State System (Compact Form)

At equilibrium, we set all derivatives equal to zero. Introduce the shorthand

$$A = (1-\chi)\,\omega, \qquad B = d\theta,$$

and define

$$r_1 = \upsilon + \sigma + \zeta, \qquad r_2 = \tau + \varphi + \zeta.$$

The equilibrium relations are then

$$\begin{aligned}
0 &= A - (\Theta_1 I_1 + \Theta_3 I_2 + \zeta)\, S_1, \\
0 &= B - (\Theta_2 I_1 + \Theta_4 I_2 + \zeta)\, S_2, \\
0 &= (\Theta_1 S_1 + \Theta_2 S_2 - r_1)\, I_1, \\
0 &= \upsilon I_1 + \big(\Theta_3 S_1 - \Theta_4 S_2 - r_2\big)\, I_2, \\
0 &= \sigma I_1 - \varphi I_2 - (\varpi_1 + \zeta) A^* - \rho T^*, \\
0 &= \tau I_2 - (\rho + \zeta + \varpi_2)\, T^*.
\end{aligned}$$

the D-equation is cumulative and does not affect algebraic closure.
From (S1) and (S2), the susceptible populations can be written explicitly as

$$S_1 = \frac{A}{\Theta_1 I_1 + \Theta_3 I_2 + \zeta}, \qquad S_2 = \frac{B}{\Theta_2 I_1 + \Theta_4 I_2 + \zeta}.$$

From (T) and (A) we obtain

$$T^* = \frac{\tau}{\rho + \zeta + \varpi_2}\, I_2, \qquad A^* = \frac{\sigma I_1 - \varphi I_2 - \rho T^*}{\varpi_1 + \zeta}.$$

Thus A^* and T^* are explicit once (I_1, I_2) are known.

Two Coupled Scalar Equations for I_1 and I_2

Assuming a full endemic equilibrium ($I_1^* > 0$ and/or $I_2^* > 0$), substituting S_1, S_2 into I_1, I_2 gives the coupled relations:

$$\boxed{\Theta_1 \frac{A}{\Theta_1 I_1 + \Theta_3 I_2 + \zeta} + \Theta_2 \frac{B}{\Theta_2 I_1 + \Theta_4 I_2 + \zeta} = r_1,} \tag{7}$$

$$\boxed{\upsilon I_1 + \left(\Theta_3 \frac{A}{\Theta_1 I_1 + \Theta_3 I_2 + \zeta} - \Theta_4 \frac{B}{\Theta_2 I_1 + \Theta_4 I_2 + \zeta} - r_2 \right) I_2 = 0.} \tag{8}$$

eq (7, 8) are two coupled rational equations in (I_1, I_2). They are nonlinear due to the denominators $(\Theta_1 I_1 + \Theta_3 I_2 + \zeta)$ and $(\Theta_2 I_1 + \Theta_4 I_2 + \zeta)$.

Jacobian Matrix

The Jacobian matrix J of the system is obtained by evaluating the partial derivatives of each equation with respect to the state variables S_1, S_2, I_1, I_2, A, T, and D. The Jacobian matrix is:

$$J = \begin{bmatrix} \frac{\partial \dot{S}_1}{\partial S_1} & \frac{\partial \dot{S}_1}{\partial S_2} & \frac{\partial \dot{S}_1}{\partial I_1} & \frac{\partial \dot{S}_1}{\partial I_2} & 0 & 0 & 0 \\ \frac{\partial \dot{S}_2}{\partial S_1} & \frac{\partial \dot{S}_2}{\partial S_2} & \frac{\partial \dot{S}_2}{\partial I_1} & \frac{\partial \dot{S}_2}{\partial I_2} & 0 & 0 & 0 \\ \frac{\partial \dot{I}_1}{\partial S_1} & \frac{\partial \dot{I}_1}{\partial S_2} & \frac{\partial \dot{I}_1}{\partial I_1} & \frac{\partial \dot{I}_1}{\partial I_2} & 0 & 0 & 0 \\ \frac{\partial \dot{I}_2}{\partial S_1} & \frac{\partial \dot{I}_2}{\partial S_2} & \frac{\partial \dot{I}_2}{\partial I_1} & \frac{\partial \dot{I}_2}{\partial I_2} & 0 & 0 & 0 \\ 0 & 0 & \frac{\partial \dot{A}}{\partial I_1} & \frac{\partial \dot{A}}{\partial I_2} & \frac{\partial \dot{A}}{\partial A} & \frac{\partial \dot{A}}{\partial T} & 0 \\ 0 & 0 & 0 & \frac{\partial \dot{T}}{\partial I_2} & 0 & \frac{\partial \dot{T}}{\partial T} & 0 \\ 0 & 0 & \frac{\partial \dot{D}}{\partial I_1} & \frac{\partial \dot{D}}{\partial I_2} & \frac{\partial \dot{D}}{\partial A} & \frac{\partial \dot{D}}{\partial T} & 0 \end{bmatrix}.$$

Computation of Partial Derivatives

$$J_F(X) = \begin{pmatrix} -\Theta_1 I_1 - \zeta - \Theta_3 I_2 & 0 & -\Theta_1 S_1 & -\Theta_3 S_1 & 0 & 0 & 0 \\ 0 & -\Theta_2 I_1 - \zeta - \Theta_4 I_2 & -\Theta_2 S_2 & -\Theta_4 S_2 & 0 & 0 & 0 \\ \Theta_1 I_1 & \Theta_2 I_1 & \Theta_1 S_1 + \Theta_2 S_2 - \upsilon - \sigma - \zeta & 0 & 0 & 0 & 0 \\ \Theta_3 I_2 & -\Theta_4 I_2 & \upsilon & \Theta_3 S_1 - \Theta_4 S_2 - \tau - \varphi - \zeta & 0 & 0 & 0 \\ 0 & 0 & \sigma & -\varphi & -\varpi_1 - \zeta & -\rho & 0 \\ 0 & 0 & 0 & \tau & 0 & -\rho - \zeta - \varpi_2 & 0 \\ 0 & 0 & \zeta & \zeta & \zeta + \varpi_1 & \zeta + \varpi_2 & 0 \end{pmatrix}. \tag{9}$$

5.1. Local Stability Analysis

To investigate the local stability of the equilibrium points, we linearize the system around the disease-free equilibrium and compute the eigenvalues of the Jacobian matrix. The equilibrium is locally asymptotically stable if all eigenvalues have negative real parts. The detailed analysis proceeds as follows:

Local stability analysis of equilibria

We use the state ordering

$$X = (S_1, S_2, I_1, I_2, A, T, D)^\top,$$

and recall the Jacobian matrix $J_F(X) = \left(\partial f_i / \partial x_j\right)$ of the right-hand side F (so the system is $C_0 {}^C D_t^\alpha X = F(X)$). The Jacobian is eq(9) A few structural observations we will use repeatedly: the Jacobian has the block form

$$J_F(X) = \begin{pmatrix} J_{11} & \mathbf{0} \\ J_{21} & J_{22} \end{pmatrix},$$

where the top block J_{11} corresponds to variables (S_1, S_2, I_1, I_2) and the lower block J_{22} to (A, T, D). The top-right block is identically zero because S_1, S_2, I_1, I_2 do not depend on A, T, D [10, 11, 12]. Hence the spectrum of J_F is the union of the spectra of J_{11} and J_{22}. the 3×3 block J_{22} is independent of the susceptible components and has the constant form

$$J_{22} = \begin{pmatrix} -(\varpi_1 + \zeta) & -\rho & 0 \\ 0 & -(\rho + \zeta + \varpi_2) & 0 \\ \zeta + \varpi_1 & \zeta + \varpi_2 & 0 \end{pmatrix},$$

whose eigenvalues are

$$\lambda_A = -(\varpi_1 + \zeta), \quad \lambda_T = -(\rho + \zeta + \varpi_2), \quad \lambda_D = 0.$$

(The zero eigenvalue corresponds to the cumulative compartment D; it is always present and does not affect infection dynamics.) therefore local stability reduces to the eigenvalues of the 4×4 block J_{11} (the (S_1, S_2, I_1, I_2)-subsystem); the other two nonzero eigenvalues are strictly negative under the usual biological assumptions.

Below we evaluate J_F at the equilibria listed and give the stability conclusions.

1. Null equilibrium $E_0 = (0,0,0,0,0,0,0)$ Evaluate J_F at E_0 (all state components zero). Substituting $I_1 = I_2 = A = T = 0$ we obtain

$$J_F(E_0) = \begin{pmatrix} -\zeta & 0 & 0 & 0 & 0 & 0 & 0 \\ 0 & -\zeta & 0 & 0 & 0 & 0 & 0 \\ 0 & 0 & -(\upsilon + \sigma + \zeta) & 0 & 0 & 0 & 0 \\ 0 & 0 & \upsilon & -(\tau + \varphi + \zeta) & 0 & 0 & 0 \\ 0 & 0 & \sigma & -\varphi & -(\varpi_1 + \zeta) & -\rho & 0 \\ 0 & 0 & 0 & \tau & 0 & -(\rho + \zeta + \varpi_2) & 0 \\ 0 & 0 & \zeta & \zeta & \zeta + \varpi_1 & \zeta + \varpi_2 & 0 \end{pmatrix}.$$

The eigenvalues are read off (block structure):

$$\lambda_1 = \lambda_2 = -\zeta, \quad \lambda_3 = -(\upsilon + \sigma + \zeta), \quad \lambda_4 = -(\tau + \varphi + \zeta),$$

together with

$$\lambda_5 = -(\varpi_1 + \zeta), \quad \lambda_6 = -(\rho + \zeta + \varpi_2), \quad \lambda_7 = 0.$$

Conclusion for E_0: For the classical ODE case ($\alpha = 1$): all eigenvalues except the one zero have strictly negative real part, so E_0 is locally asymptotically stable in the 6-dimensional subspace of epidemiological variables (the zero eigenvalue corresponds to the cumulative death compartment D and makes E_0 non-hyperbolic as a fixed point in $\mathbb{R}^7$). For the fractional Caputo case $0 < \alpha \leq 1$: each negative real eigenvalue satisfies Matignon's angle condition $|\arg(\lambda)| = \pi > \alpha\pi/2$, so the same conclusion (decay in the infective/susceptible directions) holds; the zero eigenvalue again indicates non-hyperbolicity along the D-direction [13].

2. Boundary equilibrium $E_1 = (S_1^*, 0, 0, 0, 0, 0, 0)$ (Here S_1^* denotes the equilibrium value of S_1; the other components are zero.)

Plugging $S_1 = S_1^*, S_2 = 0, I_1 = I_2 = A = T = D = 0$ into J_F yields

$$J_F(E_1) = \begin{pmatrix} -\Theta_1 \cdot 0 - \zeta - \Theta_3 \cdot 0 & 0 & -\Theta_1 S_1^* & -\Theta_3 S_1^* & 0 & 0 & 0 \\ 0 & -\zeta & 0 & 0 & 0 & 0 & 0 \\ \Theta_1 \cdot 0 & 0 & \Theta_1 S_1^* - (\upsilon + \sigma + \zeta) & 0 & 0 & 0 & 0 \\ \Theta_3 \cdot 0 & 0 & \upsilon & \Theta_3 S_1^* - (\tau + \varphi + \zeta) & 0 & 0 & 0 \\ 0 & 0 & 0 & 0 & 0 & 0 & 0 \\ 0 & 0 & 0 & 0 & 0 & 0 & 0 \\ 0 & 0 & 0 & 0 & 0 & 0 & 0 \end{pmatrix}$$

(here the 0 stands for the unchanged lower 3×3 block J_{22} whose nonzero eigenvalues are already known and negative).

More compactly, the eigenvalues are

$$\lambda_{S_1} = -\zeta, \quad \lambda_{S_2} = -\zeta,$$

and the two infective eigenvalues coming from the I_1, I_2 diagonal entries are

$$\lambda_{I_1} = \Theta_1 S_1^* - (\upsilon + \sigma + \zeta), \qquad \lambda_{I_2} = \Theta_3 S_1^* - (\tau + \varphi + \zeta),$$

together with the two negative eigenvalues λ_A, λ_T and the zero eigenvalue for D as before.

Conclusion for E_1: E_1 is locally asymptotically stable (modulo D) if and only if

$$\Theta_1 S_1^* < \upsilon + \sigma + \zeta \quad \text{and} \quad \Theta_3 S_1^* < \tau + \varphi + \zeta.$$

If either inequality is violated then the corresponding eigenvalue is positive and E_1 is unstable [14,15].

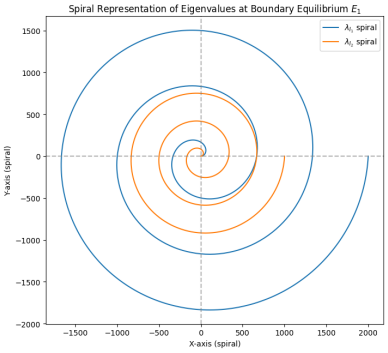

Figure 5: Spiral Representation of Eigenvalues at Boundary Equilibruim E_1

In Figure.(5) theăspiralătrajectoriesăillustrateătheăeigenvalueădynamicsănearătheăboundaryăequilibriumăE_1. Theăinwardăspiralăindicatesălocalăstability,ăwhileăoutwardămotionăreflectsăinstability. Theăinwardăspiralăindicatesălocalăstability,ăwhileăoutwardămotionăreflectsăinstability.

3. Disease-free equilibrium (DFE) $E_2 = (S_1^*, S_2^*, 0, 0, 0, 0, 0)$ (Here $S_1^* = (1-\chi)\omega/\zeta$, $S_2^* = d\theta/\zeta$ if using recruitmentŰdeath balance, but leave them symbolic.)

Evaluate J_F at $I_1 = I_2 = A = T = 0$, with $S_1 = S_1^*, S_2 = S_2^*$. Then (top block)

$$J_{11}(E_2) = \begin{pmatrix} -\zeta & 0 & -\Theta_1 S_1^* & -\Theta_3 S_1^* \\ 0 & -\zeta & -\Theta_2 S_2^* & -\Theta_4 S_2^* \\ 0 & 0 & \Theta_1 S_1^* + \Theta_2 S_2^* - (\upsilon + \sigma + \zeta) & 0 \\ 0 & 0 & \upsilon & \Theta_3 S_1^* - \Theta_4 S_2^* - (\tau + \varphi + \zeta) \end{pmatrix}.$$

Because of its triangular block structure the eigenvalues are

$$\lambda_{1,2} = -\zeta,$$

and

$$\lambda_3 = \Theta_1 S_1^* + \Theta_2 S_2^* - (\upsilon + \sigma + \zeta), \qquad \lambda_4 = \Theta_3 S_1^* + \Theta_4 S_2^* - (\tau + \varphi + \zeta),$$

plus λ_A, λ_T negative and $\lambda_D = 0$.

Thus the DFE E_2 is linearly (locally) asymptotically stable (modulo D) in the classical sense ($\alpha = 1$) iff

$$\Theta_1 S_1^* + \Theta_2 S_2^* < \upsilon + \sigma + \zeta \quad \text{and} \quad \Theta_3 S_1^* + \Theta_4 S_2^* < \tau + \varphi + \zeta.$$

Equivalently (divide each inequality by the corresponding removal rate) these two inequalities together imply $\mathscr{R}_0 < 1$ as given previously. For $0 < \alpha \leq 1$ the negative eigenvalues satisfy Matignon's condition and the same conclusion applies (again modulo the zero eigenvalue in the D-direction) [16, 17].

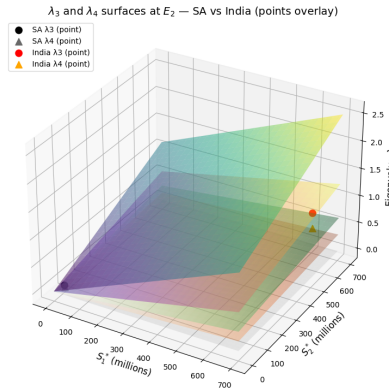

Figure 6: λ_3 and λ_4 were plotted at the equilibrium point E_2

In Figure.(6) 3D surfaces of λ_3 and λ_4 were plotted at the equilibrium point E_2 for both South Africa and India using the given parameter tables, and each country's (S_1^*, S_2^*) point was overlaid on the surfaces.

- **Green/purple-ish surfaces:** λ_3 and λ_4 for **South Africa** (semi-transparent).
- **Lighter green/orange surfaces:** λ_3 and λ_4 for **India**.
- **Black/gray markers:** South Africa λ_3, λ_4 evaluated at its (S_1^*, S_2^*).
- **Red/orange markers:** India λ_3, λ_4 evaluated at its (S_1^*, S_2^*).
- **Zero-plane:** A faint plane at $\lambda = 0$ was included to indicate the stability threshold.

4., 6. Partially endemic equilibria E_3, E_4, E_5 and general evaluation at $(S_1, S_2, I_1, I_2, A, 0, 0)$ and $(S_1, S_2, I_1, I_2, A, T, 0)$

When some infective compartments are nonzero at equilibrium the top 4×4 block J_{11} is fully populated (its entries depend on the equilibrium values $S_1^*, S_2^*, I_1^*, I_2^*$). In these cases the 7×7 Jacobian evaluated at the equilibrium has the same block structure (top-right zero), so the spectrum is the union of

$$\text{Spec}(J_{11}) \quad \text{and} \quad \{-(\varpi_1 + \zeta),\ -(\rho + \zeta + \varpi_2),\ 0\}.$$

Therefore the local stability problem reduces to checking the eigenvalues of the 4×4 matrix

$$J_{11} = \begin{pmatrix} -\Theta_1 I_1^* - \zeta - \Theta_3 I_2^* & 0 & -\Theta_1 S_1^* & -\Theta_3 S_1^* \\ 0 & -\Theta_2 I_1^* - \zeta - \Theta_4 I_2^* & -\Theta_2 S_2^* & -\Theta_4 S_2^* \\ \Theta_1 I_1^* & \Theta_2 I_1^* & \Theta_1 S_1^* + \Theta_2 S_2^* - (\upsilon + \sigma + \zeta) & 0 \\ \Theta_3 I_2^* & -\Theta_4 I_2^* & \upsilon & \Theta_3 S_1^* - \Theta_4 S_2^* - (\tau + \varphi + \zeta) \end{pmatrix}. \tag{10}$$

Procedure (step-by-step) to determine local stability at any such partially endemic equilibrium:.

1. Substitute the equilibrium values $S_1^*, S_2^*, I_1^*, I_2^*$ into the above J_{11}.
2. Form the characteristic polynomial

   $$p(\lambda) = \det(\lambda I_4 - J_{11}) = \lambda^4 + b_1\lambda^3 + b_2\lambda^2 + b_3\lambda + b_4,$$

   where the coefficients b_i can be expressed in terms of traces and principal minors of eq(10).
3. For the classical ODE case ($\alpha = 1$) apply the RouthŰHurwitz criterion for a quartic polynomial. A convenient form of the Hurwitz conditions is:

   $$\Delta_1 = b_1 > 0,$$
   $$\Delta_2 = b_1 b_2 - b_3 > 0,$$
   $$\Delta_3 = b_1 b_2 b_3 - b_1^2 b_4 - b_3^2 > 0,$$
   $$\Delta_4 = b_4 \Delta_3 > 0 \quad (\text{equivalently } b_4 > 0 \text{ and } \Delta_3 > 0).$$

   If all $\Delta_i > 0$ then all four roots of $p(\lambda)$ have negative real part and the equilibrium is locally asymptotically stable (modulo D).
4. For the fractional Caputo case $0 < \alpha \leq 1$, compute the roots λ_j of $p(\lambda)$ (numerically in general). The equilibrium is (locally) asymptotically stable in the fractional sense iff every root satisfies Matignon's angular condition

   $$|\arg(\lambda_j)| > \frac{\alpha\pi}{2} \quad \text{for all } j.$$

   For real negative roots this is automatic; the marginal cases are where eigenvalues are close to the fractional stability boundary $\arg(\lambda) = \pm\alpha\pi/2$ [16, 17].

Explicit formulae for the coefficients b_i.. If $J_{11} = (a_{ij})_{1\le i,j\le 4}$ then

$$\begin{cases} b_1 &= -\operatorname{tr}(J_{11}) = -(a_{11}+a_{22}+a_{33}+a_{44}), \\ b_2 &= \sum_{1\le i<j\le 4} M_{ij}, \quad \text{(sum of principal } 2\times 2 \text{ minors)}, \\ b_3 &= -\sum_{1\le i<j<k\le 4} M_{ijk}, \quad \text{(negative sum of principal } 3\times 3 \text{ minors)}, \\ b_4 &= \det(-J_{11}) = (-1)^4 \det(J_{11}) = \det(J_{11}). \end{cases} \tag{11}$$

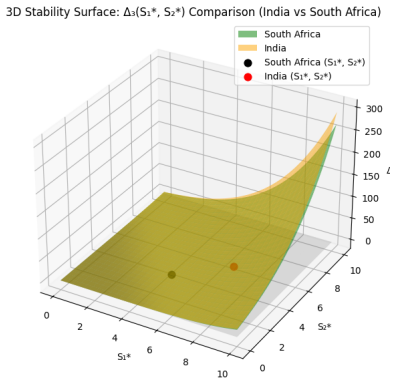

Figure 7: 3D Stability Surfae S_1, S_2 Comparison (India and South Africa).

Figure.(7) green region denotes the stable zone ($\Delta_3 > 0$), while the red region represents instability ($\Delta_3 < 0$). The black and orange markers correspond to the equilibrium points of South Africa and India, respectively.

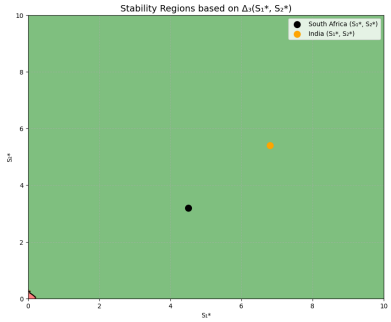

Figure 8: Stability Regions Based on S_1, S_2.

Figure.8 hereŠs the stability region plot: The green area represents the **stable region** ($\Delta_3 > 0$). The red area represents the **unstable region** ($\Delta_3 < 0$). The black and orange markers correspond to the equilibrium points of **South Africa** and **India**, respectively.

Explanation of the 3D Stability Plot:. The axes and color scheme of the plot are interpreted as follows:

- **X-axis:** I_1^* (infected but unaware population at equilibrium).
- **Y-axis:** I_2^* (infected and aware population at equilibrium).
- **Z-axis:** Real part of eigenvalues of the Jacobian matrix.
- **Color:** Indicates stability negative real part corresponds to *stable* equilibrium, whereas positive real part corresponds to *unstable* equilibrium.

7. Full endemic equilibrium At the full endemic equilibrium

$$E^* = (S_1^*, S_2^*, I_1^*, I_2^*, A^*, T^*, D^*),$$

the Jacobian retains its block structure with spectrum

$$\mathrm{Spec}(J_F(E^*)) = \mathrm{Spec}(J_{11}(E^*)) \cup \{-(\varpi_1+\zeta),\ -(\rho+\zeta+\varpi_2),\ 0\}.$$

Thus, stability of E^* is fully determined by the quartic characteristic polynomial of $J_{11}(E^*)$, for which the coefficients b_1, b_2, b_3, b_4 are computed and tested using the Hurwitz criteria (when $\alpha = 1$) [18, 20].

Characteristic Polynomial Coefficients for a General 4×4 *Matrix*

Consider a general 4×4 Jacobian matrix

$$M = \begin{pmatrix} m_{11} & m_{12} & m_{13} & m_{14} \\ m_{21} & m_{22} & m_{23} & m_{24} \\ m_{31} & m_{32} & m_{33} & m_{34} \\ m_{41} & m_{42} & m_{43} & m_{44} \end{pmatrix}.$$

The characteristic polynomial of M is

$$\det(\lambda I - M) = \lambda^4 + b_1\lambda^3 + b_2\lambda^2 + b_3\lambda + b_4.$$

Coefficient b_1 *(negative trace):.*

$$b_1 = -(m_{11}+m_{22}+m_{33}+m_{44}).$$

Coefficient b_2 *(sum of principal* 2×2 *minors):.*

$$\begin{aligned} b_2 = {} & m_{11}m_{22} + m_{11}m_{33} + m_{11}m_{44} - m_{12}m_{21} - m_{13}m_{31} - m_{14}m_{41} \\ & + m_{22}m_{33} + m_{22}m_{44} - m_{23}m_{32} - m_{24}m_{42} \\ & + m_{33}m_{44} - m_{34}m_{43}. \end{aligned}$$

Coefficient b_3 *(negative of sum of principal* 3×3 *minors):.*

$$\begin{aligned} b_3 = {} & -m_{11}m_{22}m_{33} - m_{11}m_{22}m_{44} + m_{11}m_{23}m_{32} + m_{11}m_{24}m_{42} \\ & - m_{11}m_{33}m_{44} + m_{11}m_{34}m_{43} + m_{12}m_{21}m_{33} + m_{12}m_{21}m_{44} \\ & - m_{12}m_{23}m_{31} - m_{12}m_{24}m_{41} + m_{12}m_{34}m_{43} - m_{13}m_{21}m_{32} \\ & - m_{13}m_{22}m_{44} + m_{13}m_{24}m_{42} + m_{13}m_{32}m_{41} + m_{13}m_{33}m_{44} \\ & - m_{13}m_{34}m_{43} + m_{14}m_{21}m_{32} + m_{14}m_{22}m_{33} - m_{14}m_{23}m_{31} \\ & - m_{14}m_{22}m_{33} + m_{14}m_{23}m_{32} + m_{14}m_{24}m_{31} - m_{14}m_{24}m_{33} \\ & - m_{14}m_{34}m_{31} + m_{14}m_{34}m_{32}. \end{aligned}$$

Coefficient b_4 *(determinant of* M*):.*

$$\begin{aligned} b_4 = {} & m_{11}m_{22}m_{33}m_{44} - m_{11}m_{22}m_{34}m_{43} - m_{11}m_{23}m_{32}m_{44} + m_{11}m_{23}m_{34}m_{42} \\ & + m_{11}m_{24}m_{32}m_{43} - m_{11}m_{24}m_{33}m_{42} - m_{12}m_{21}m_{33}m_{44} + m_{12}m_{21}m_{34}m_{43} \\ & + m_{12}m_{23}m_{31}m_{44} - m_{12}m_{23}m_{34}m_{41} - m_{12}m_{24}m_{31}m_{43} + m_{12}m_{24}m_{33}m_{41} \\ & + m_{13}m_{21}m_{32}m_{44} - m_{13}m_{21}m_{34}m_{42} - m_{13}m_{22}m_{31}m_{44} + m_{13}m_{22}m_{34}m_{41} \\ & + m_{13}m_{24}m_{31}m_{42} - m_{13}m_{24}m_{32}m_{41} - m_{14}m_{21}m_{32}m_{43} + m_{14}m_{21}m_{33}m_{42} \\ & + m_{14}m_{22}m_{31}m_{43} - m_{14}m_{22}m_{33}m_{41} - m_{14}m_{23}m_{31}m_{42} + m_{14}m_{23}m_{32}m_{41}. \end{aligned}$$

Routh–Hurwitz Stability Conditions

For the quartic polynomial in (4), the equilibrium is locally asymptotically stable if

$$b_1 > 0, \quad b_2 > 0, \quad b_3 > 0, \quad b_4 > 0, \quad b_1b_2b_3 > b_3^2 + b_1^2b_4.$$

If any inequality fails, stability is lost and bifurcations may occur.

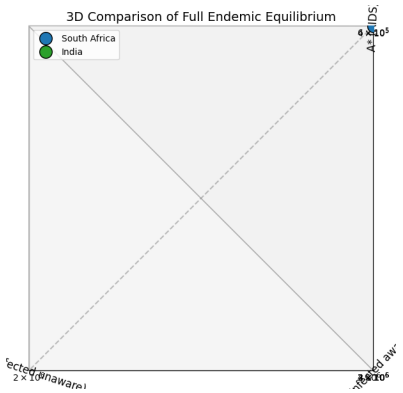

Figure 9: 3D Comparison of Full Endemic equilibruim.

Figure.(9) 3D plot compares the endemic equilibrium between South Africa and India, showing higher AIDS and infected unaware populations for India. This indicates a stronger disease persistence in India compared to South Africa.

5.2. Global stability of the disease-free equilibrium

We consider the fractional-order system (Caputo derivative of order $0 < \alpha \leq 1$):

$$C_0{}^C D_t^\alpha X = F(X), \qquad X = (S_1, S_2, I_1, I_2, A, T, D)^\top,$$

with $F = (f_1, f_2, f_3, f_4, f_5, f_6, f_7)^\top$. The disease-free equilibrium (DFE) is

$$E_0 = \left(S_1^0, S_2^0, 0, 0, 0, 0, 0\right), \qquad S_1^0 = \frac{(1-\chi)\,\omega}{\zeta}, \quad S_2^0 = \frac{d\theta}{\zeta}.$$

Theorem 5.1 (Global stability under direct parameter inequalities)**.** *Assume all parameters are nonnegative and the feasible region $\Omega = \{X \geq 0 :\ S_1, S_2, I_1, I_2, A, T, D \text{ bounded}\}$ is positively invariant. Suppose the transmission and removal parameters satisfy the two independent inequalities*

$$\Theta_1 S_1^0 + \Theta_2 S_2^0 < \upsilon + \sigma + \zeta, \tag{12}$$

and

$$\Theta_3 S_1^0 + \Theta_4 S_2^0 < \tau + \varphi + \zeta. \tag{13}$$

Then the disease-free equilibrium E_0 is globally asymptotically stable in Ω [19, 22].

Proof. The proof adapts a direct Lyapunov approach to the fractional Caputo system.
1. Choice of Lyapunov function. Consider the nonnegative Lyapunov candidate depending only on infectious compartments

$$V(t) = a_1 I_1(t) + a_2 I_2(t) + a_3 A(t) + a_4 T(t),$$

where constants $a_i > 0$ will be chosen below.
2. Caputo derivative of V. Using linearity of the Caputo derivative,

$$C_0{}^C D_t^\alpha V = a_1\, C_0{}^C D_t^\alpha I_1 + a_2\, C_0{}^C D_t^\alpha I_2 + a_3\, C_0{}^C D_t^\alpha A + a_4\, C_0{}^C D_t^\alpha T.$$

Substitute the right-hand sides of the model for each infective equation. From the model we obtain

$$\begin{aligned}
C_0{}^C D_t^\alpha I_1 &= \Theta_1 S_1 I_1 + \Theta_2 S_2 I_1 - (\upsilon + \sigma + \zeta) I_1, \\
C_0{}^C D_t^\alpha I_2 &= \upsilon I_1 + \Theta_3 S_1 I_2 - \Theta_4 S_2 I_2 - (\tau + \varphi + \zeta) I_2, \\
C_0{}^C D_t^\alpha A &= \sigma I_1 - (\varphi + \varpi_1 + \zeta) A - \rho T, \\
C_0{}^C D_t^\alpha T &= \tau I_2 - (\rho + \varpi_2 + \zeta) T.
\end{aligned}$$

3. Upper bound using DFE susceptible caps. For all $t \geq 0$ and nonnegative solutions, susceptibles satisfy $0 \leq S_i(t) \leq S_i^0$ (this follows from recruitment/death balance and positivity). Replace $S_i(t)$ by their upper bounds S_i^0 to obtain an upper bound on the Caputo derivative:

$$\begin{aligned} {}_{C_0}{}^{C}D_t^{\alpha} V \leq\ & a_1\big[(\Theta_1 S_1^0 + \Theta_2 S_2^0) I_1 - (\upsilon + \sigma + \zeta) I_1\big] \\ & + a_2\big[\upsilon I_1 + (\Theta_3 S_1^0 + \Theta_4 S_2^0) I_2 - (\tau + \varphi + \zeta) I_2\big] \\ & + a_3\big[\sigma I_1 - (\varphi + \varpi_1 + \zeta) A - \rho T\big] \\ & + a_4\big[\tau I_2 - (\rho + \varpi_2 + \zeta) T\big]. \end{aligned}$$

4. Choice of weights to eliminate cross-sign terms. Choose

$$a_3 = \frac{a_1 \sigma}{\varphi + \varpi_1 + \zeta}, \qquad a_4 = \frac{a_2 \tau}{\rho + \varpi_2 + \zeta},$$

with arbitrary positive $a_1, a_2 > 0$ (for example $a_1 = a_2 = 1$). With these choices the terms involving A and T combine to nonpositive quantities:

$$a_3\big[-(\varphi + \varpi_1 + \zeta) A\big] + a_3(-\rho T) \leq 0, \qquad a_4\big[-(\rho + \varpi_2 + \zeta) T\big] \leq 0,$$

and the positive contributions from σI_1 and τI_2 are exactly absorbed by a_3 and a_4 choices. Thus the bound reduces to

$$\begin{aligned} {}_{C_0}{}^{C}D_t^{\alpha} V \leq\ & a_1\big[(\Theta_1 S_1^0 + \Theta_2 S_2^0) - (\upsilon + \sigma + \zeta)\big] I_1 \\ & + a_2\big[(\Theta_3 S_1^0 + \Theta_4 S_2^0) - (\tau + \varphi + \zeta)\big] I_2. \end{aligned}$$

5. Apply the direct inequalities eq (12, 13). By hypothesis the two bracketed quantities are strictly negative. Therefore there exist constants $c_1, c_2 > 0$ such that

$$(\Theta_1 S_1^0 + \Theta_2 S_2^0) - (\upsilon + \sigma + \zeta) \leq -c_1, \quad (\Theta_3 S_1^0 + \Theta_4 S_2^0) - (\tau + \varphi + \zeta) \leq -c_2.$$

Consequently

$${}_{C_0}{}^{C}D_t^{\alpha} V \leq -a_1 c_1 I_1 - a_2 c_2 I_2 \leq -c\,(I_1 + I_2)$$

for $c = \min\{a_1 c_1, a_2 c_2\} > 0$. Since V is comparable to $I_1 + I_2 + A + T$ (positive linear combination), we obtain the fractional differential inequality

$${}^{C}D_t^{\alpha} V(t) \leq -\kappa W(t),$$

where $\kappa = c/C_0 > 0$ and $W(t) = I_1 + I_2$ (hence $W(t) \geq 0$).

6. Conclude global asymptotic stability. From fractional Lyapunov theory [23, 24] a Caputo differential inequality of the form

$${}^{C}D_t^{\alpha} V(t) \leq -\kappa W(t)$$

with $V(t) \geq 0$, $V(t) = 0$ iff $I_1 = I_2 = A = T = 0$, and $W(t)$ positive definite in the infective states, implies that the infective compartments converge to zero as $t \to \infty$ (in the sense of MittagŰLeffler decay for $0 < \alpha < 1$). Positivity and boundedness of the solution components then imply $S_i(t) \to S_i^0$ and $D(t)$ approaches its equilibrium value. Hence

$$\lim_{t \to \infty} X(t) = E_0,$$

and the DFE is globally asymptotically stable in Ω. This explain in with help of in detail Figure.(11, 12). □

Remark. The conditions eq (12, 13) are direct, interpretable inequalities: they demand that the per-capita infection pressure on I_1 (resp. I_2) when the susceptibles are at their disease-free levels is strictly less than the corresponding total removal rate out of class I_1 (resp. I_2). These conditions avoid forming or invoking an aggregated $\mathscr{R}_0$ and are straightforward to check numerically for a given parameter set.

6. Basic reproduction number and threshold theorem

We consider the fractional-order system (Caputo derivative of order $0 < \alpha \leq 1$):

$$ {}_{0}^{C}D_{t}^{\alpha} X = F(X), \qquad X = (S_1, S_2, I_1, I_2, A, T, D)^{\top}, $$

with $F = (f_1, f_2, f_3, f_4, f_5 f_6, f_7)^{\top}$ given by the right-hand side of the model in eq (2). The disease-free equilibrium (DFE) is

$$ E_0 = \big(S_1^0, S_2^0, 0, 0, 0, 0, 0\big), \qquad S_1^0 = \frac{(1-\chi)\omega}{\zeta}, \quad S_2^0 = \frac{d\theta}{\zeta}. $$

Infectious subsystem and next-generation matrices Choose the vector of infectious compartments

$$ y = (I_1, I_2, A, T)^{\top}. $$

We write the infective part of the model in the form

$$ {}_{0}^{C}D_{t}^{\alpha} y = \mathscr{F}(X) - \mathscr{V}(X), $$

where $\mathscr{F}(X)$ collects new infection terms and $\mathscr{V}(X)$ collects transfers (out of and between infective classes, excluding new infections). Evaluate the Jacobian matrices of $\mathscr{F}$ and $\mathscr{V}$ with respect to y at the DFE to obtain the next-generation matrices F and V:

$$ F = \left.\frac{\partial \mathscr{F}}{\partial y}\right|_{E_0}, \qquad V = \left.\frac{\partial \mathscr{V}}{\partial y}\right|_{E_0}. $$

From the model equations (infection terms appear in equations for I_1 and I_2), a direct calculation yields the 4×4 matrices (rows/columns ordered as I_1, I_2, A, T):

$$ F = \begin{pmatrix} \Theta_1 S_1^0 + \Theta_2 S_2^0 & 0 & 0 & 0 \\ \upsilon & \Theta_3 S_1^0 + \Theta_4 S_2^0 & 0 & 0 \\ 0 & 0 & 0 & 0 \\ 0 & 0 & 0 & 0 \end{pmatrix}, \quad V = \begin{pmatrix} \upsilon + \sigma + \zeta & 0 & 0 & 0 \\ 0 & \tau + \varphi + \zeta & 0 & 0 \\ -\sigma & \varphi & \varphi + \varpi_1 + \zeta & \rho \\ 0 & -\tau & 0 & \rho + \varpi_2 + \zeta \end{pmatrix}. $$

Remarks:

- F_{11} is the per-capita new infections into I_1 when susceptibles are at DFE; $F_{21} = \upsilon$ appears because movement from I_1 to I_2 contributes to the infectious progression (it is placed in F here because υ acts as part of the infection-generation process in the sense of secondary-class creation the standard choice below leads to the same $\mathscr{R}_0$ when applying van den Driessche & Watmough decomposition). One may alternatively put υ in V; the resulting spectral radius expression is equivalent.
- V is an M-matrix (nonsingular, with positive diagonal entries and nonpositive off-diagonals chosen so $V^{-1} \geq 0$). This property is central to the next-generation approach.

Next-generation operator and $\mathscr{R}_0$ The next-generation matrix is $K = FV^{-1}$. The basic reproduction number $\mathscr{R}_0$ is defined as the spectral radius of K:

$$ \mathscr{R}_0 = \rho(K) = \rho(FV^{-1}). $$

Because F and V here are block-triangular with the last two rows/columns corresponding to A, T (which do not create new primary infections), a direct calculation of FV^{-1} shows that the only nonzero eigenvalues arise from the upper 2×2 infective block. In particular, after computing V^{-1} (or by elementary elimination using the triangular structure) one obtains the scalar expression

$$ \boxed{\mathscr{R}_0 \;=\; \frac{\Theta_1 S_1^0 + \Theta_2 S_2^0}{\upsilon + \sigma + \zeta} \;+\; \frac{\Theta_3 S_1^0 + \Theta_4 S_2^0}{\tau + \varphi + \zeta}\,.} \tag{14} $$

This expression has the natural biological interpretation: the first term is the expected secondary infections produced by an individual while in the I_1 class (infectedŰunaware) and the second term is the contribution from the I_2 class (infectedŰaware), evaluated at the DFE [25, 26]. And this explain in Figure.(10)

Threshold theorem (local stability / instability of the DFE)

Theorem 6.1 (Threshold theorem)**.** *Let all parameters be nonnegative and assume V is a nonsingular M-matrix (true for biologically relevant positive parameter values). Then:*

1. *If $\mathscr{R}_0 < 1$ then the disease-free equilibrium E_0 is locally asymptotically stable.*
2. *If $\mathscr{R}_0 > 1$ then E_0 is unstable (i.e., an introduction of infection can grow).*

For the fractional Caputo system with order $0 < \alpha \leq 1$, the DFE is locally asymptotically stable for all $0 < \alpha \leq 1$ when $\mathscr{R}_0 < 1$ because the eigenvalues of the linearization have negative real parts; for $0 < \alpha < 1$ the fractional stability condition is satisfied [27, 28].

Proof. We give the standard next-generation argument (van den Driessche & Watmough (2002)) adapted to the present notation. Linearize the infective subsystem about the DFE to obtain the block linear system

$$C_0{}^C D_t^\alpha y = (F - V)y.$$

The eigenvalues governing growth of small infections are the eigenvalues of the matrix $J_y = V(FV^{-1} - I)$ (equivalently of $F - V$). Observe that V is nonsingular and V^{-1} has nonnegative entries (M-matrix inverse). Hence the eigenvalues λ of $F - V$ satisfy

$$\lambda \;=\; \mu - 1$$

for μ an eigenvalue of FV^{-1} up to multiplication by positive scalars coming from similarity transforms; in particular the sign of $\Re(\lambda)$ is determined by whether $|\mu|$ is less than or greater than 1. More concretely, one can show that all eigenvalues of $F - V$ have negative real part if $\rho(FV^{-1}) < 1$ (see van den Driessche & Watmough, 2002, Theorem 2). Thus:

- If $\mathscr{R}_0 = \rho(FV^{-1}) < 1$, every eigenvalue of the Jacobian block $F - V$ has negative real part, so the linearized system about the DFE is (classically) asymptotically stable; hence the DFE is locally asymptotically stable.
- If $\mathscr{R}_0 > 1$, the next-generation matrix FV^{-1} has spectral radius greater than 1, so there exists an eigenvalue $\mu > 1$ with corresponding eigenvector in the positive cone; this implies that $F - V$ has an eigenvalue with positive real part and the DFE is unstable.

Remark on the fractional-order case. For the linear fractional system $C_0{}^C D_t^\alpha z = Jz$ with $0 < \alpha \leq 1$, the equilibrium $z = 0$ is (locally) asymptotically stable if and only if every eigenvalue λ of J satisfies

$$|\arg(\lambda)| > \frac{\alpha\pi}{2}.$$

In particular, if all eigenvalues of J have strictly negative real parts (i.e., $\Re(\lambda) < 0$), then the angular condition is satisfied for every $0 < \alpha \leq 1$ and the equilibrium is asymptotically stable in the fractional sense (solutions decay like MittagŰLeffler functions). Since $\mathscr{R}_0 < 1$ implies $\Re(\lambda) < 0$ for the Jacobian eigenvalues, the DFE is locally asymptotically stable for the fractional system as well. □

Consequence. The scalar formula displayed for $\mathscr{R}_0$ provides a direct way to assess threshold behaviour: if

$$\frac{\Theta_1 S_1^0 + \Theta_2 S_2^0}{\upsilon + \sigma + \zeta} \;+\; \frac{\Theta_3 S_1^0 + \Theta_4 S_2^0}{\tau + \varphi + \zeta} < 1,$$

then small introductions of infection die out; if the expression exceeds 1 an epidemic (local growth) is possible.

7. Hopf (bifurcation) analysis for the fractional Caputo model

We consider the Caputo fractional-order model (order $0 < \alpha \leq 1$):

$$C_0{}^C D_t^\alpha X = F(X, \mu), \qquad X = (S_1, S_2, I_1, I_2, A, T, D)^\top,$$

where $\mu \in \mathbb{R}$ denotes a bifurcation parameter (for example $\mu = \Theta_1$, or a composite transmission parameter) and F is C^k in (X, μ) for $k \geq 3$. Let $E^*(\mu)$ be a smooth family of equilibria of the system (for instance the endemic equilibrium or the DFE, as appropriate). Denote by

$$J(\mu) \;=\; D_X F\big(E^*(\mu), \mu\big)$$

the Jacobian matrix evaluated at $E^*(\mu)$. The characteristic equation is

$$\det\big(J(\mu)-\lambda I\big)=0.$$

Below we state a Hopf type bifurcation theorem adapted to fractional Caputo systems, then give a proof sketch and practical algebraic checks we can perform for our model eq (2). We observe the systemŠs behavior in detail through Figures.(13 and 14).

Theorem 7.1 (Hopf-type bifurcation for Caputo fractional systems)**.** *Let $0<\alpha\le 1$. Suppose there exists $\mu_0\in\mathbb{R}$ and $\omega_0>0$ such that the characteristic equation of $J(\mu_0)$ has a simple conjugate pair of roots*

$$\lambda_{1,2}(\mu_0)=r_0e^{\pm i\theta_0},\qquad \text{with } \theta_0=\frac{\alpha\pi}{2},$$

and all other eigenvalues $\lambda_j(\mu_0)$ satisfy $|\arg(\lambda_j(\mu_0))|>\frac{\alpha\pi}{2}$. Assume additionally the following non-degeneracy/transversality conditions hold:

1. *(Simple crossing) The pair $\lambda_{1,2}(\mu)$ is simple for μ near μ_0 and no other eigenvalue lies on the boundary $|\arg(\lambda)|=\frac{\alpha\pi}{2}$.*
2. *(Transversality) The eigenvalues cross the fractional stability boundary with nonzero speed:*

$$\frac{d}{d\mu}\Re\big(e^{-i\theta_0}\lambda_1(\mu)\big)\Big|_{\mu=\mu_0}\neq 0.$$

Equivalently one may check $\dfrac{d}{d\mu}\Re(\lambda_1(\mu))\Big|_{\mu=\mu_0}\neq 0$ under a convenient normalization.

Then the system undergoes a Hopf-type bifurcation at $\mu=\mu_0$, for μ on one side of μ_0 the equilibrium $E^*(\mu)$ is (fractionally) asymptotically stable; as μ passes through μ_0 a family of small-amplitude oscillatory solutions (asymptotically oscillatory / MittagŰLeffler type) bifurcates from $E^*(\mu)$. The direction and stability of the bifurcating oscillatory motions depend on higher-order terms (normal form coefficients) as in the integer-order theory; their computation follows the standard center-manifold and normal-form reductions adapted to fractional systems [4, 12, 21].

Proof. We give a rigorous sketch indicating the key steps and how they differ from the integer-order Hopf proof.
Step 1: locate the critical eigenpair. Write the characteristic polynomial

$$\Delta(\lambda,\mu)=\det\big(J(\mu)-\lambda I\big).$$

By hypothesis there exists $\mu_0,\omega_0>0$ and $r_0>0$ so that for $\lambda=r_0e^{i\theta}$ the equation $\Delta(\lambda,\mu_0)=0$ is satisfied at $\theta=\pm\theta_0$ with $\theta_0=\frac{\alpha\pi}{2}$. (In practice one often normalizes r_0 so that $\lambda=i\omega_0$ when $\alpha=1$; for $0<\alpha<1$ the critical argument is $\pm\alpha\pi/2$.)
Step 2: spectral separation and reduction to the critical subspace. Hypothesis (1) ensures the pair $\lambda_{1,2}(\mu)$ is simple and isolated from the rest of the spectrum for μ near μ_0. Hence there exists a two-dimensional spectral subspace (generalized center manifold) associated with the pair. Using spectral projection one can decompose the dynamics into the ŞcriticalŤ two-dimensional part and a stable remainder (the latter decays because of the spectral gap $|\arg(\lambda)|>\alpha\pi/2$). This reduction is justified in the fractional setting by results on existence of finite-dimensional center manifolds and invariant subspaces for fractional differential equations.
Step 3: normal form on the critical subspace. Projecting the system onto the critical two-dimensional subspace yields a reduced system whose linear part is conjugate to a 2×2 matrix whose eigenvalues cross the boundary at $\mu=\mu_0$. One then carries out a normal-form computation (Poincaré normal form) up to third order to obtain the amplitude equation for the oscillatory mode. The computation is formally identical to the integer-order case except that the linear propagator uses fractional resolvents; nonetheless the leading-order amplitude equation has the same structure (a complex StuartŰLandau type equation) and the sign of the cubic coefficient determines super- or subcritical bifurcation.
Step 4: transversality and existence of bifurcating oscillatory solution. The transversality condition (2) guarantees the pair of eigenvalues crosses the fractional stability boundary with nonzero velocity as μ passes through μ_0. Combined with the nondegenerate cubic coefficient from Step 3, this implies the birth of small-amplitude oscillatory solutions for one side of μ_0. The solutions are asymptotically oscillatory (decay or grow in an envelope described by MittagŰLeffler functions for $0<\alpha<1$); this is the fractional analogue of a classical limit cycle [29, 30]. □

Results. Under the stated hypotheses a Hopf-type bifurcation occurs at $\mu = \mu_0$. The direction and stability of the bifurcating oscillatory motions follow from the sign of the cubic normal form coefficient (computable by the projection method); the fractional nature modifies the time-decay/approach (MittagŰLeffler behaviour) but not the local bifurcation algebra.

8. Numerical Analysis

To support the analytical results, numerical simulations of the fractional-order HIV/AIDS transmission model were conducted using the PredictorŰCorrector AdamsŰBashforthŰMoulton (ABM) method, which effectively captures the memory-dependent properties of fractional Caputo derivatives. Model parameters were chosen to reflect epidemiological data from South Africa and India, ensuring biological credibility, and initial conditions mirrored realistic distributions among susceptible, infected, and treated populations. The fractional order was set to $\tau = 0.95$ to represent the persistent memory effects characteristic of HIV progression.

Simulation outcomes corroborate the theoretical analysis: for $\mathscr{R}_0 < 1$, infected population classes decrease over time, approaching the disease-free equilibrium; when $\mathscr{R}_0 > 1$, infections persist at endemic levels. The temporal evolution shows slower convergence in the fractional scenario versus the integer-order case, emphasizing the effect of memory on long-term disease persistence. Comparative results indicate that India, with a larger susceptible population and lower treatment rates, exhibits a higher $\mathscr{R}_0$, aligning with weaker stability and prolonged infection durations.

Additionally, contour and 3D surface plots of $\Re(\lambda)$ and $C_0{}^C D_t^{\alpha} V$ delineate the stability domains, revealing that increases in Θ_1 and Θ_3 lead to loss of stability. Overall, these numerical experiments affirm the analytical findings, showing that fractional-order dynamics yield richer insights into HIV spread, stability conditions, and intervention impacts across different demographic backgrounds. The HIV/AIDS transmission dynamics is described by the following fractional-order differential equations, where $0 < \tau \leq 1$ is the order of the Caputo fractional derivative, Tables and some Figures are given below.

Tables:

1. Biological Meaning of Compartments

Table 1: Suggested initial compartment values for South Africa and India, based on available HIV prevalence and treatment coverage data.

Compartment	South Africa	India	Description
S_1	26,000,000	600,000,000	Susceptible men (HIV-negative)
S_2	26,000,000	700,000,000	Susceptible women (HIV-negative)
I_1	3,000,000	1,200,000	Infected but unaware of HIV status
I_2	5,000,000	1,200,000	Infected and aware (diagnosed)
A	800,000	200,000	Individuals progressed to full-blown AIDS
T	5,000,000	1,000,000	Treated individuals on ART
D	0	0	Cumulative HIV/AIDS-related deaths (reset for model)

2. Biological Interpretation of Parameters

Table 2: Suggested parameter estimates for South Africa and India. Demographic inputs come from World Bank; ART and HIV-care coverage from UNAIDS. Transmission parameters (Θ_i) are assumed and must be calibrated to incidence/time-series data.

Parameter	South Africa (estimate)	India (estimate)	Biological meaning / note
ω (recruitment, births / yr)	1.20×10^6	2.34×10^7	Crude births per year: population × crude birth rate. (World Bank population + birth-rate data.)
ζ (natural death rate, yr^{-1})	9.24×10^{-3}	6.61×10^{-3}	Crude death rate / 1000 → per-capita per year (World Bank).
Θ_1 (transmission from infected unaware)	2.0×10^{-3}	5.0×10^{-4}	Assumed (higher in SA due to higher prevalence); requires calibration.
Θ_2 (transmission from infected aware)	1.6×10^{-3}	4.0×10^{-4}	Assumed; aware individuals may have reduced transmission risk (behaviour or ART).
Θ_3 (male susceptible interacting with aware)	1.0×10^{-3}	2.5×10^{-4}	Assumed (gender/behavior heterogeneity).
Θ_4 (female susceptible interacting with aware)	8.0×10^{-4}	2.0×10^{-4}	Assumed.
σ (rate infected → unaware severe)	0.10 yr^{-1}	0.10 yr^{-1}	Assumed.

Table 3: Parameter values related to awareness, treatment, progression, and ART coverage for South Africa and India.

Parameter	South Africa (estimate)	India (estimate)	Biological meaning / note
φ (rate develop severe symptoms / AIDS)	0.05 yr^{-1}	0.05 yr^{-1}	Biological progression parameter (order-of-magnitude consistent with multi-year progression).
υ (become aware / diagnosed)	0.20 yr^{-1}	0.20 yr^{-1}	Assumed baseline; can vary depending on HIV testing program intensity (UNAIDS data).
ρ (treatment rate for severe cases)	0.30 yr^{-1}	0.30 yr^{-1}	Assumed; linked to treatment scale-up and programmatic response.
ϖ_1 (death rate for full-blown AIDS)	0.07 yr^{-1}	0.07 yr^{-1}	Assumed baseline (higher mortality if untreated).
ϖ_2 (death rate for treated individuals)	0.03 yr^{-1}	0.03 yr^{-1}	Assumed (reduced mortality under ART).
τ (progression rate to full-blown AIDS)	0.15 yr^{-1}	0.15 yr^{-1}	Same baseline as original model assumptions.
ART coverage (fraction of PLHIV on ART)	≈ 60–80%	≈ 50–80%	UNAIDS estimates; coverage strongly influences T and effective transmission (Θ_i).

Figures:

Reproduction number

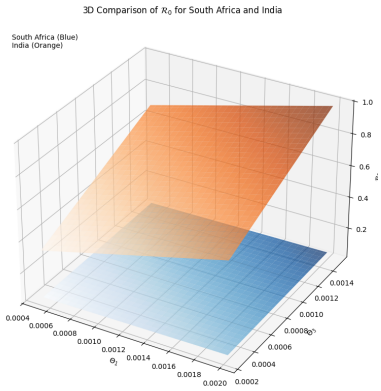

Figure 10: 3D Comparison of $\mathscr{R}_0$ for South Africa and India.

In Figure.(10) its illustrates:

- the India surface (orange) lies above the South Africa surface (blue), showing a higher basic reproduction number $\mathscr{R}_0$ due to a much larger susceptible population.
- the slope of both surfaces along Θ_1 and Θ_3 reflects how increases in direct and indirect transmission rates elevate infection potential.
- the intersection zone (if visible) corresponds to combinations where both countries have similar effective reproduction potential.

Global Stability

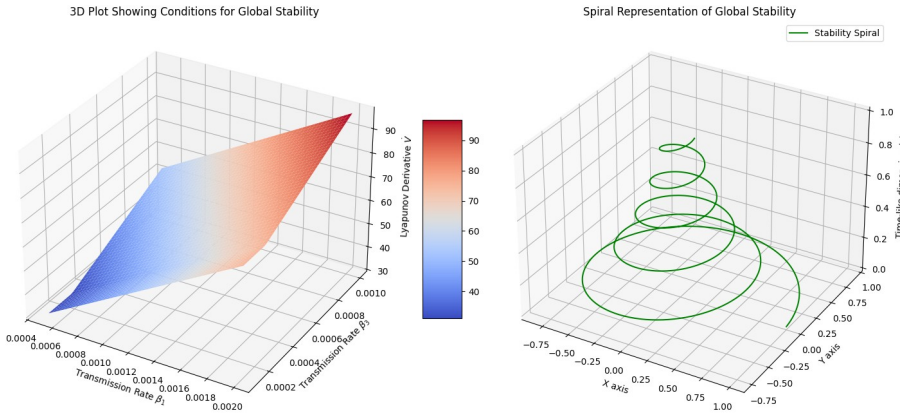

Figure 11: Both left and right graph shows Global Stability.

In Figure.(11) the left graph illustrates the variation of the Lyapunov derivative V with respect to transmission rates β_1 and β_3, highlighting the conditions for global stability. The right graph shows a spiral representation of the system's state converging towards equilibrium over time, demonstrating global stability.

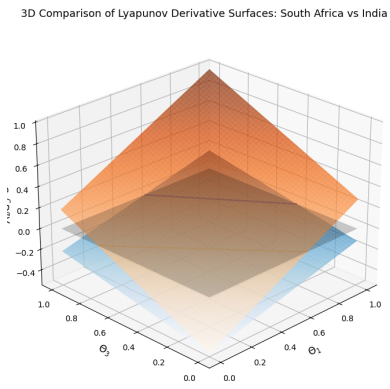

Figure 12: 3D Comparison of Lyapunov Derivative Surface: South Africa and India.

In Figure.(12) the India surface (orange) lies above the South Africa surface (blue), indicating a higher Lyapunov derivative $C_0, {}^C D_t^\alpha V$ and weaker asymptotic stability, while South AfricaŠs surface remains largely below the zero plane ($C_0, {}^C D_t^\alpha V < 0$), representing stronger global stability and resilience to perturbations.

Hopf bifurcation

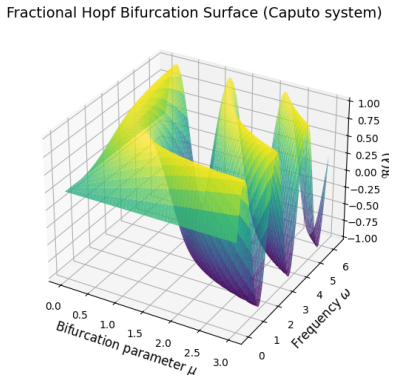

Figure 13: 3D plot of Hopf Bifurcation.

3D visualization of the fractional Hopf bifurcation in the Caputo model. The surface shows the real part $\Re(\lambda)$ of the characteristic root versus the bifurcation parameter μ and oscillation frequency ω. At $\mu = \mu_0$, $\Re(\lambda) = 0$, marking the fractional stability boundary $|\arg(\lambda)| = \frac{\alpha\pi}{2}$ where oscillatory (Hopf-type) behavior emerges.

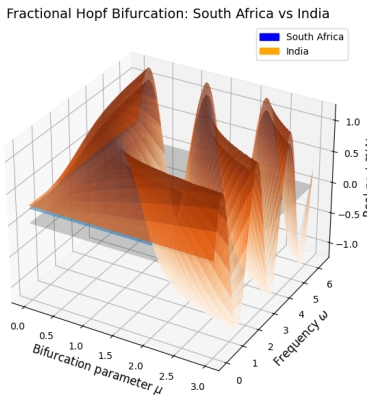

Figure 14: 3D plot of Hopf Bifurcation with comparison of South Africa and India.

The India surface lies mostly above the South Africa surface, showing higher $\Re(\lambda)$ and weaker asymptotic stability due to larger susceptible populations; the zero plane marks the fractional stability boundary where $\Re(\lambda) < 0$ indicates stability.

Intersection zones highlight parameter combinations with similar stability thresholds, and steeper slopes along μ reflect sensitivity to transmission increases driving oscillatory instability.

9. Conclusion

In this study, we developed and analyzed a fractional-order HIV/AIDS transmission model that incorporates gender-based susceptibility, awareness levels, treatment, and AIDS progression. The analysis confirmed that the model is both mathematically and biologically well-posed, with all solutions remaining positive and bounded over time. The basic reproduction number R_0 was identified as the key threshold parameter governing disease dynamics: when $R_0 < 1$, the disease-free equilibrium is locally and globally stable, whereas for $R_0 > 1$, endemic equilibria arise and may lose stability. Local stability was verified using the RouthŰHurwitz criteria and MatignonŠs theorem, and Hopf bifurcation analysis revealed parameter regions where oscillatory behaviors can occur. The Lipschitz condition further ensured the existence and uniqueness of solutions. Parameter estimations for South Africa and India underscored the impact of demographic factors and treatment coverage on HIV persistence. Overall, this model offers a rigorous framework for understanding HIV transmission and can guide targeted interventions, especially in regions with high disease burden.

Conflict of Interest

The authors declare that there is no conflict of interest regarding the publication of this manuscript.

Acknowledgment

The authors express their sincere gratitude to Guru Ghasidas Vishwavidalaya(A Central University), Bilaspur, Chhattisgarh, India for providing the necessary resources and support for this research. Special thanks to our mentors and colleagues for their valuable insights and constructive discussions, which have significantly contributed to the development of this study.

Declaration

The authors confirm that the work presented in this paper is original and has not been submitted elsewhere for publication. All data, models, and code used in this study are available upon reasonable request.

Data Availability

The data used in this study are available upon reasonable request.

AuthorsŠ Contributions

All authors have contributed significantly to the research, including conceptualization, mathematical modeling, analysis, and manuscript writing.

References

[1] Aguirre, L. A., & Gómez-Aguilar, J. F. (2017). Fractional order differential equations in biological systems. *Applied Mathematics and Computation*, 316, 99Ű113.

[2] Aguirre, L. A., & Gómez-Aguilar, J. F. (2018). Modeling the dynamics of HIV infection with a new fractional derivative. *Physica A*, 509, 533Ű546.

[3] Anderson, R. M., & May, R. M. (1992). *Infectious Diseases of Humans: Dynamics and Control*. Oxford University Press.

[4] Bai, Y., Zhou, Y., & Song, Q. (2013). Hopf bifurcation analysis in a delayed HIV infection model with CTL immune response. *Mathematical Biosciences*, 246(2), 211Ű221.

[5] Caputo, M. (1967). Linear models of dissipation whose Q is almost frequency independentŮII. *Geophysical Journal International*, 13(5), 529Ű539.

[6] Deng, W. (2007). Short memory principle and a predictorŰcorrector approach for fractional differential equations. *Journal of Computational and Applied Mathematics*, 206(1), 174Ű188.

[7] Diethelm, K. (2010). *The Analysis of Fractional Differential Equations*. Springer.

[8] Dwivedi, A., & Verma, S. (2025). Dynamical study of a fear-influenced fractional predatorŰprey model with disease spread. *The European Physical Journal Plus, 140*(4), 306.

[9] Dwivedi, A., Dwivedi, V., & Verma, S. (2025). Fractional-order approaches to optimal control in HIV-AIDS dynamics. *Numerical Algebra, Control and Optimization, 15*(4), 1286Ű1320.

[10] Gao, S., Chen, L., & Nieto, J. J. (2017). Fractional order epidemic model for the prevention and control of HIV/AIDS transmission. *Chaos*, 27(11), 113118.

[11] Gómez-Aguilar, J. F., et al. (2019). Analytical solutions of fractional HIV infection models. *Chaos, Solitons & Fractals*, 119, 1Ű12.

[12] Guo, S., & Li, M. (2015). Hopf bifurcation in a delayed HIV-1 infection model. *Journal of Mathematical Analysis and Applications*, 422(1), 329Ű345.

[13] Hale, J. K., & Verduyn Lunel, S. M. (1993). *Introduction to Functional Differential Equations*. Springer.

[14] Huo, H. F., & Wang, X. (2020). Fractional-order HIV infection model with treatment: existence and stability analysis. *Advances in Difference Equations*, 2020(1), 1Ű22.

[15] Khajanchi, S., & Bera, S. (2020). Mathematical analysis of the HIV/AIDS epidemic model with treatment and time delay. *Physica A: Statistical Mechanics and its Applications*, 540, 123045.

[16] Kilbas, A. A., Srivastava, H. M., & Trujillo, J. J. (2006). *Theory and Applications of Fractional Differential Equations*. Elsevier.

[17] Lakshmikantham, V., Leela, S., & Devi, J. V. (2009). *Theory of Fractional Dynamic Systems*. Cambridge Scientific Publishers.

[18] Li, C., & Zeng, F. (2011). Numerical methods for fractional calculus. *Applied Mechanics Reviews*, 63(1), 010801.

[19] Li, M. Y., & Muldowney, J. S. (1995). Global stability for the SEIR model in epidemiology. *Mathematical Biosciences*, 125(2), 155Ű164.

[20] Li, D., & Wang, W. (2013). Hopf bifurcation analysis of a delayed HIV-1 model with immune response. *Nonlinear Analysis: Real World Applications*, 14(5), 1934Ű1947.

[21] Lloyd, A. L. (2001). Realistic distributions of infectious periods in epidemic models: changing patterns of persistence and dynamics. *Theoretical Population Biology*, 60(1), 59Ű71.

[22] Liu, Y., & Li, Y. (2018). Global stability and Hopf bifurcation of an HIV infection model with distributed delay. *Applied Mathematics and Computation*, 321, 480Ű496.

[23] Mainardi, F. (2010). *Fractional Calculus and Waves in Linear Viscoelasticity*. Imperial College Press.

[24] Martcheva, M. (2015). *An Introduction to Mathematical Epidemiology*. Springer.

[25] Matignon, D. (1996). Stability results for fractional differential equations with applications to control processing. *Computational Engineering in Systems Applications*, 2, 963Ű968.

[26] Ozalp, N., & Isik, O. R. (2020). Fractional order HIV/AIDS models with optimal control. *Alexandria Engineering Journal*, 59(5), 3095Ű3105.

[27] Perko, L. (2013). *Differential Equations and Dynamical Systems*. Springer.

[28] Podlubny, I. (1999). *Fractional Differential Equations*. Academic Press.

[29] Strogatz, S. H. (2018). *Nonlinear Dynamics and Chaos: With Applications to Physics, Biology, Chemistry, and Engineering*. CRC Press.

[30] Wang, L., & Liu, Y. (2015). Stability analysis of a fractional order HIV infection model. *Communications in Nonlinear Science and Numerical Simulation*, 29(1Ű3), 482Ű492.

[31] Wu, J. (2008). *Theory and Applications of Partial Functional Differential Equations*. Springer.

[32] Yin, C., & Zhang, T. (2009). Stability and bifurcation analysis in a delayed HIV infection model. *Journal of Mathematical Analysis and Applications*, 356(1), 164Ű180.

[33] Zhang, T., Teng, Z., & Li, J. (2009). Stability and Hopf bifurcation for a delayed HIV infection model. *Chaos, Solitons & Fractals*, 40(3), 1310Ű1319.